Journal of Chemical Neuroanatomy 90 (2018) 87–97

Contents lists available at ScienceDirect

Journal of Chemical Neuroanatomy

journal homepage: www.elsevier.com/locate/jchemneu

Cortical and spinal conditioned media modify the inward ion currents and excitability and promote differentiation of human striatal primordium

Eglantina Idrizaj[a], Erica Sarchielli[b], Annamaria Morelli[b], Rachele Garella[a], Maria Caterina Baccari[a], Pasquale Gallina[c], Gabriella Barbara Vannelli[b], Fabio Francini[a], Roberta Squecco[a,*]

[a] Department of Experimental Clinical Medicine, University of Florence, Section of Physiological Sciences, Viale GB Morgagni 63, 50134, Florence, Italy
[b] Department of Experimental Clinical Medicine, University of Florence, Section of Anatomy and Histology, Largo Brambilla 3, 50134, Florence, Italy
[c] Department of Surgery and Translational Medicine, Neurosurgery School of Tuscany, University of Florence, Largo Brambilla 3, 50134, Florence, Italy

ARTICLE INFO

Keywords:
Human striatal primordium
Conditioned media
Immunofluorence
Electrophysiology

ABSTRACT

Human striatal precursor cells (HSPs) isolated from ganglionic eminence may differentiate in electrophysiologically functional excitable neuron-like cells and a number of endogenous molecules such as hormones, neurotransmitters or growth factors can actually regulate neuronal growing and differentiation. The purpose of this research was to assess, by electrophysiological and immunocytochemical analysis, if the type of culture medium could specifically impact on the neuronal differentiation potential of HSPs. Accordingly, HSPs were maintained in different inductive media such as cortical and spinal cord conditioned media, and we estimated the possible changes in the main ion currents, excitability and expression of neuronal markers indicative of neuronal differentiation. Our results have shown that 36 h exposure to each of the conditioned media, with their blend of autocrine and paracrine growth factors, was able to modify significantly the electrophysiological membrane properties and the functional expression of inward ionic currents in selected neuronal HSPs. Moreover, although both types of conditioned media determined neuronal maturation (increased neuritogenesis and increased expression of neuronal and striatal markers), each of them leads to the occurrence of different functional features. Particularly, the spinal medium caused a stronger depolarization of the membrane potential and significantly increased the amplitude of Na^+ current as well as L- and N- type Ca^{2+} currents, definitely modifying their kinetics. In contrast, the cortical medium mainly caused a significant and more marked increase of the membrane conductance and time constant values. These results strongly support the plasticity of our cellular model that, although already committed towards a specific phenotype, it can be differently affected by the conditioned media, thereby resulting functionally modifiable according to environmental cues.

1. Introduction

After many years of numerous slightly effective studies on neural transplantation in animal models and clinical trials, we are now cautiously approaching to successful treatment of the damaged brain and related syndromes. Among the different neurodegenerative diseases, Huntington's disease (HD) is a rare incurable heritable disorder characterized by progressive death of medium size spiny neurons within the striatum, a basal ganglia structure (Novak and Tabrizi, 2010). In this regard, the replacement of degenerated striatum and repair of circuitries by grafting fetal striatal primordium has been imagined as a strategy to treat HD (Peschanski et al., 1995). Indeed, fetal neural tissue transplants are being exploited in human neurodegenerative diseases (Clelland et al., 2008) as a first step for a broader strategy of molecular and cellular therapies, being the best substitutes one could imagine. In fact, neuronal precursor cells can actually retain the ability to develop into the different neuronal cells found in the adult brain. If the any improvement could be consistently replicated and the benefits last for a

Abbreviations: BDNF, brain-derived neurotrophic factor; C_m, cell capacitance; CM, cortical medium; FGF2, fibroblast growth factor 2; G_m, resting membrane conductance; G_m/C_m, membrane specific conductance; G_{max}, maximal conductance for the activating current; G_{max}/C, $_{mm}$maximal specific conductance; HD, Huntington's disease; HP, holding potential; HSP, human striatal precursor; HVA, high voltage-activated Ca^{2+} currents; I_a, activating current; I_{Ca}, Ca^{2+} currents; I, $_{Camax}/C_m$current specific maximal size; I_p/C_m, normalized peak current; I_m, steady-state membrane current; I_{Na}, Na^+ currents; I_{tot}/C_m, specific total Ca^{2+} current trace; k_a, steepness factor for activation curve; k_h, steepness factor for inactivation curve; LVA, low voltage-activated Ca^{2+} currents; R, $_{aa}$access resistance; R_i, input resistance; R_m, membrane resistance; RMP, resting membrane potential; SM, spinal medium; τ, time constant of the transient's decay; V_a, potential eliciting the half-maximal activation; V_h, potential eliciting the half-maximal inactivation; V_{rev}, apparent reversal potential

* Corresponding author at: Department of Experimental and Clinical Medicine, Section of Physiological Sciences, University of Florence, Viale GB Morgagni 63, 50134 Florence, Italy.
E-mail address: roberta.squecco@unifi.it (R. Squecco).

https://doi.org/10.1016/j.jchemneu.2017.12.005
Received 2 August 2017; Received in revised form 19 December 2017; Accepted 19 December 2017
Available online 20 December 2017
0891-0618/

reasonable period without complications, a clinical treatment might develop using fetal precursor cells. In the recent years, a few clinical reports have suggested that transplantation of human fetal striatal tissue in HD patients may lead to effective improvement of the symptoms (Pauly et al., 2012). Accordingly, HD patients were grafted with striatal primordium from 9 to 12 week old human fetuses, and the analysis of the outcome demonstrated that transplantation positively affected the clinical course providing a prolonged cognitive and motor benefit, which paralleled the graft survival, development and function (Gallina et al., 2010; Paganini et al., 2014). The striatal primordium originates in the ganglionic eminence (Ulfig, 2000) and the striatal neuronal precursors divide, migrate, and differentiate establishing connections responsible for the basal ganglia circuits (Evans et al., 2012). A better comprehension of the mechanisms underlying normal striatal ontogenesis may be central to any improvement of cell-based therapies since we imagined that the grafted striatal primordium continued its ontogenesis in the host, restoring functions and mitigating neurodegeneration through either cell replacement, endogenous repair, or trophic support.

We have previously reported that human striatal precursor cells (HSPs) isolated from ganglionic eminence are a mixed population including immature elements, neuronal/glial-restricted progenitors and mature striatal neurons, and possess the machinery for long-term survival, proliferation and differentiation (Sarchielli et al., 2014; Ambrosini et al., 2015). Moreover, HSPs may differentiate in electrophysiologically functional excitable neuron-like cells (n-HSP) (Squecco et al., 2016). However, *in vivo*, various external factors such as hormones, neurotransmitters or peptides (growth factors) regulate neuronal growth, migration and differentiation (Sariola and Saarma, 2003; Moody and Bosma, 2005; Bouron et al., 2006; Zuccato et al., 2010; Yuzwa et al., 2016). Indeed, the surrounding environment and the factors released therein may be determinant in inducing those specific mechanisms that regulate the fate and maturation of precursor cells.

The aim of this *in vitro* research was to assess further the neuronal differentiation potential of HSPs into functional n-HSPs and to evaluate whether this potential could be influenced by the conditioned medium of cell preparations obtained from two different districts of the central nervous system: cerebral cortex and spinal cord. To this end, we used the cortical conditioned medium to investigate HSPs differentiation potential based on the known influence that cortical input may have in the striatum during the brain development (Plotkin et al., 2005). As well, since the spinal cord is the downstream effector of the striatal control, we also investigated whether during fetal development extrinsic factors derived from spinal cord neurons could affect HSP differentiation potential. We have previously shown that certain neurotrophins such as brain-derived neurotrophic factor (BDNF) and fibroblast growth factor 2 (FGF2) are able to significantly increase neuronal differentiation and neurite length of HSPs (Sarchielli et al., 2014), as well as the functional acquisition of typical neuronal Ca^{2+} currents (Squecco et al., 2016). In the present study, we investigated whether cortical and spinal conditioned media, with their blend of growth and signalling autocrine and paracrine factors, were able to modify significantly and in a qualitatively different manner, the morpho-functional features of n-HSPs in terms of inward ionic currents expression, excitability and neuronal differentiation phenotype.

2. Materials and methods

2.1. Cell cultures

Neuronal samples were obtained as previously described (Gallina et al., 2010) from three (9–12 week old) legally aborted fetuses, according to the ethical guidelines of the Italian National Institute of Health. The use of human fetal tissue for research purposes was approved by the National Ethics Committee and the Committee for investigation in Humans of the University of Florence (Protocol n° 678304). From each fetus, HSPs, frontal-parietal cortex and spinal cord primary cultures were obtained and propagated *in vitro*, as previously described (Crescioli et al., 2008; Sarchielli et al., 2014). Briefly, tissue fragments of 0.5–1 mm were incubated with 1 mg/ml collagenase (type IV) for enzymatic digestion. The cell suspensions were mechanically dispersed by pipetting in Coon's modified Ham's F12 medium supplemented with 10% FBS. The cells were seeded in plastic dishes and incubated at 37 °C in 5% CO_2 atmosphere. By using EDTA–trypsin solution, the confluent cells were split to 1:2–1:4 ratio. Cells at passages 3/4 were systematically used for the experiments: 10^5 of HSPs cells were plated onto coverslips, serum starved for 24 h at 37 °C, and then subjected to electrophysiological analysis. The serum-free Coon's modified Ham's F12 medium was here referred to as control medium. In a parallel set of experiments, HSP cells were cultured for 36 h in a conditioned medium resulting from the primary culture of cortical neurons (cortical medium, CM), spinal cord neurons (spinal medium, SM), obtained from the same fetus, and then analyzed. Both CM and SM were collected after that cortical or spinal cells, respectively, were plated in plain medium (Coon's modified Ham's F12 medium supplemented with 10% FBS) and left to reach confluence (5–7 days). The resulting culture medium was mixed 1:1 with fresh Coon's modified Ham's F12 medium and used to treat HSP cells. The conditioned media were screened for pH values that resulted 8.78 and 8.45 for CM and SM, respectively.

2.2. Immunofluorescence analysis

Immunofluorescence analysis was performed as previously described (Sarchielli et al., 2014; Ambrosini et al., 2015). Briefly, the cells grown on sterile slides were fixed in 3.7% paraformaldehyde in phosphate buffered saline (PBS) for 15′ at room temperature, followed by permeabilization in PBS containing 0.1% Triton X-100 for 10′. Immunostaining was performed with anti-glial fibrillary acidic protein (GFAP, 1:100; Santa Cruz Biotechnology, Santa Cruz, CA, USA), anti-NeuN (1:100, Millipore Corp., Bedford, USA), anti-nestin (1:100, Millipore Corp.), anti β tubulin III (1:50, Santa Cruz) and anti MAP2 (1:100, Millipore Corp.), followed by Alexa Fluor 568 goat anti-rabbit or Alexa Fluor 488 goat anti-mouse IgG (H + L) (1:200; Molecular Probes, Eugene, OR, USA). Antibody specificity was verified by omitting the primary antibody.

2.3. Western blotting analysis

Western blot analysis was performed as previously described (Sarchielli et al., 2014). Briefly, HSP cells were grown in F12 Coon's, treated with conditioned media and lysed in standard lysis buffer supplemented with protease inhibitor cocktail (Sigma Aldrich, Saint Louis, MO, USA). Aliquots containing 20 µg of proteins were loaded on SDS-PAGE, then transferred on poly-vinylidene difluoride membranes, blocked in 3% BSA and incubated with the following primary antibodies: anti-DARPP32 (1:1000, Sigma Aldrich) and anti-β actin (1:10000, Santa Cruz). The incubation with the primary antibodies was followed by peroxidase conjugated secondary IgG treatment and the reacted proteins were revealed by the enhanced chemiluminescence system (ECL extend, Euroclone, Milan, Italy). Image acquisition and densitometric analysis were performed with Quantity One software on a ChemiDoc XRS instrument (Bio-Rad Laboratories Inc.) and using β actin for normalization.

2.4. Electrophysiology

Low-resistance patch pipettes (3–7 MΩ) were made from borosilicate glass tubing (Harvard apparatus LTD) using a vertical puller (Narishige, Tokyo, Japan) and were used for whole-cell voltage-clamp recordings. Recording pipettes were filled with a pipette solution that contained (mM): 150 CsBr, 5 $MgCl_2$, 10 EGTA and 10 HEPES. pH 7.2, with KOH. Coverslips with the adherent cells maintained in control

medium (24 h) or in the conditioned media (36 h) extracted from culture of cortical neurons, CM, or of spinal neurons, SM, were superfused at a rate of 1.8 ml min^{-1} with a physiological bath solution having the following composition (mM): 150 NaCl, 5 KCl, 2.5 $CaCl_2$, 1 $MgCl_2$, 10 D-glucose and 10 HEPES (pH 7.4 with NaOH). To test the high voltage activated Na^+ channels sensitivity, we used TTX (1 μM). To avoid the occurrence of outward K^+ currents, experiments were performed in a 20 mM-TEA bath solution (mM): 122.5 NaCl, 2 $CaCl_2$, 20 TEA-OH and 10 HEPES. To record only Ca^{2+} currents we used a Na^+- and K^+-free solution, namely a TEA-Ca^{2+} bath solution, containing (mM): 10 $CaCl_2$, 145 TEABr and 10 HEPES. Nifedipine (Sigma) was diluted at 10^{-2} M in DMSO and stored at 4 °C; it was used at 1 μM to avoid the occurrence of the high voltage activated (HVA) L-type Ca^+ currents; Ni^{2+} (200 μM) to block T-type current and Cd^{2+} (100 μM) to block all HVA Ca^{2+} currents, such as N-, R- and P/Q-type. To specifically block N-type channels, ω-conotoxin-GVIA (ω-CTx-GVIA) (Alomone Labs, Jerusalem, Israel) was diluted in distilled water at 500 μM, stored at 20 °C and used at 500 nM. All the drugs were prepared daily from stock solutions, just before use. To prevent degradation during the experiments nifedipine was stored in the dark and toxins at 4 °C.

The whole-cell configuration was obtained after gentle application of negative pressure. Access resistance was continuously monitored during the experiments. Only those cells in which access resistance (changes < 10%) was stable were included in the analysis. Pclamp6 (Axon Instruments, Foster City, CA) software was used for analysis. The technique, set up and electronics are as described in details in Squecco et al. (2016). Briefly, the patch pipette was connected to a micromanipulator and an Axopatch 200 B amplifier (Axon Instruments). Current −and Voltage-clamp protocol generation and data acquisition were controlled by using an output and an input of the A/D-D/A interfaces (Digidata 1200; Axon Instruments) and Pclamp 9 software (Axon Instruments). Currents were low-pass filtered with a Bessel filter at 2 KHz. For activation protocol the cell was held at −80 mV and step pulses, 1 s long, from −80 to 50 mV were applied in 10 mV steps. The sampling time of the early part of the current traces (up to 50 ms) was 50 μs to better observe the activation latency and the rising time of the fast Na^+ and T-type Ca^{2+} currents. Starting from 50 ms up to the end, the sampling time was increased to 10 ms in order to reduce the device memory, since a maximum number of experimental points can be sampled for each pulse protocol. In any figure, to easily distinguish superimposing traces, we depicted in bold the current traces evoked from −80 mV up to the voltage eliciting the maximal current amplitude, whereas the remaining traces up to 50 mV are thin. The voltage eliciting the maximal current amplitude is indicated next to the related current response for each panel in each figure.

For inactivation protocol a voltage test step to −20 mV were prepulsed by a protocol as that for activation, inter-pulse interval 10 ms for I_{Na} and 500 ms for I_{Ca}. Capacitive and leak currents were subtracted by the P4 procedure.

The steady-state ionic current activation was evaluated by

$$I_a(V) = G_{max}\ (V\text{-}V_{rev})/\{1 + \exp[(V_a\text{-}V)/k_a]\} \quad (1)$$

and the steady-state inactivation by

$$I_h(V) = I/\{1 + \exp[-(V_h\text{-}V)/k_h]\}, \quad (2)$$

where G_{max} is the maximal conductance for the I_a, V_{rev} is the apparent reversal potential, V_a and V_h are the potentials eliciting the half-maximal size, k_a and k_h are the steepness factors.

Electrode capacitance was compensated before disrupting the patch. The resting membrane potential (RMP) was measured by switching to the current clamp mode (I = 0) of the 200 B amplifier. The passive properties parameters were estimated as in previous work (Di Franco et al., 2016; Squecco et al., 2016). Access resistance (R_a) was not compensated for monitoring membrane area. Series resistance was compensated up to 70 ± 90%. The area beneath the capacitive transient and the time constant of the transient's decay (τ) were used to calculate the cell linear capacitance (C_m) (see also Sartiani et al., 2007) and R_a from $\tau = R_aC_m$. The measurement of membrane resistance (R_m) were corrected for R_a and was calculated from the steady-state membrane current (I_m) using the relation: $R_m = (\Delta V\text{-}I_mR_a)/I_m$, where ΔV is the command voltage step amplitude. The ratio $1/R_m$, that is the membrane conductance G_m, was used as an index of the resting cell permeability. C_m, was used as an index of the cell surface area assuming that membrane-specific capacitance is constant at 1 μF/cm^2. The membrane conductance G_m were normalized to cell linear capacitance (C_m) to allow comparison between different cells. The ratio G_m/C_m is then proposed as specific conductance. Input resistance was measured in current clamp mode in response to small 500 ms-long current pulses applied at resting membrane potential (Gustafson et al., 2006). All the experiments were performed at room temperature (22 °C).

Results from multiple experiments are expressed as mean ± SEM. Significance of differences between means was tested using Student's t test. Values of $p < 0.05$ were considered statistically significant. For multiple comparisons, one-way ANOVA with repeated measures was utilized. In any case, only selected n-HSP were included in the statistical analysis (Squecco et al., 2016). Although the whole primary cell culture resulted mainly composed of neuronal progenitors (Sarchielli et al., 2014), the chosen cells had to display inward voltage-dependent ion currents (to elude stem cells that normally don't show such currents) (Heubach et al., 2004; Li et al., 2005; Moe et al., 2005)), $R_i > 100$ MΩ and a membrane time constant > 10 ms, to exclude glial cells that have generally $R_i < 100$ MΩ and a time constant definitely < 10 ms (Westerlund et al., 2003).

3. Results

3.1. Cell morphology of n-HSP cells

HSP cells showed apparent morphological changes in time, as already described in a previous study from our research group (Sarchielli et al., 2014). Within 24–48 h from seeding, the isolated cells began to attach and grow as monolayer having a round shape. These first adherent cells became spindle-shaped within 2nd–3rd passage (P), as examined by phase contrast microscopy. At the later passages, the cells acquired a spindle-shape with extending cytoplasmic processes (P5/6). A more mature, neuronal-like phenotype was observed along with time (P8/15). The selected n-HSP cells used in the present research were at passages 3/4 and systematically showed inward Na^+ and Ca^{2+} currents. A representative image of patched cells is shown in Fig. 1A. Although they were able to elicit a single action potential, they were not capable to elicit repetitive firing. Moreover, they are actually neuron-like cells in an early differentiation stage (Onorati et al., 2014; Picken Bahrey and Moody, 2003) since they showed only T-, L- and N-type Ca^{2+} current of a small amplitude (see below).

3.2. Characterization of human fetal primary cultures of fronto-parietal cortex and spinal cord cells

In order to characterize the cell composition of cortical and spinal cord primary cultures, we performed immunofluorescence analysis. Both primary cultures exhibited a prominent neuronal component being almost completely positive for the neuronal marker NeuN (> 90%), while few cells were positive for the glial marker GFAP (< 3%) (Fig. 2).

3.3. Characterization of HSPs and the effects of the conditioned media on their phenotype

In agreement with previous data (Sarchielli etl. 2014), HSPs left in control culture medium (Ctrl) were mainly positive for the neuronal marker β-Tubulin III (63.1 ± 3.5%) and at a lower extent for the

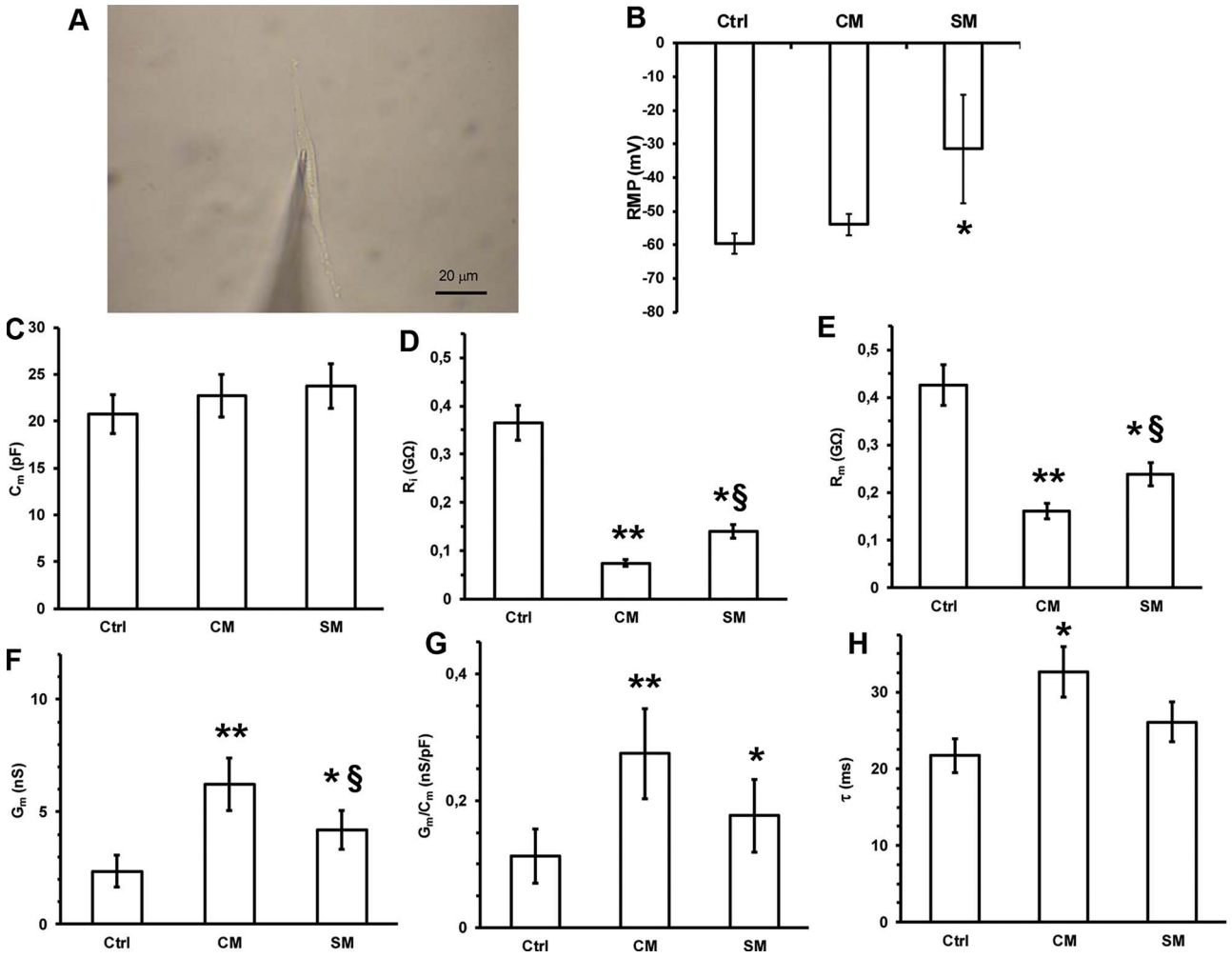

Fig. 1. Electrophysiological analysis of n-HSP membrane passive properties and effects of the conditioned media.
A) Representative patched n-HSP cell in Ctrl condition (scale bar 20 µm, magnification 40×). Effects of conditioned media on RMP (B), membrane capacitance, C_m (C), input resistance R_i (D), membrane resistance, R_m (E), resting membrane conductance, G_m (F), on the specific conductance, G_m/C_m (G), and membrane time constant, τ (H). Data are means ± SEM. * and ** indicate $p < 0.05$ and $p < 0.01$ *vs* the related control (Ctrl). §, $p < 0.05$ SM *vs* CM. In each experimental condition, data are from 34 to 38 cells.

immature neural stem cell marker nestin (21.9 ± 2.8%), as assessed by immunocytochemistry (Fig. 3A-B). Interestingly, exposing cells to CM and SM for 36 h significantly reduced the percentage of nestin-positive cells (CM, 15.0 ± 1.5%, $p < 0.05$ SM, 12.5 ± 1.2%; $p < 0.01$, Fig. 3A), while significantly increased that of cells positive for β-Tubulin III (CM, 84.0 ± 7.2%; SM, 79.8 ± 9.3%; $p < 0.05$, Fig. 3B). In addition we also detected a high percentage of cells positive for the mature neuronal marker MAP2 (55.1 ± 5.7%), which in contrast was not modified by the treatment with either CM (47.8 ± 4.1%) or SM (56.6 ± 3.8%). However, we observed a significant modification of

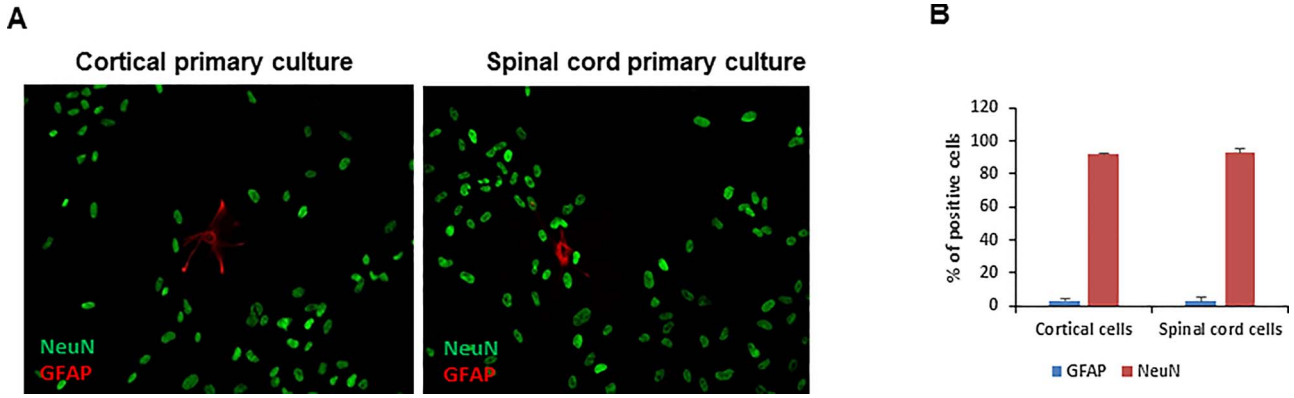

Fig. 2. Immunocytochemical phenotype characterization of primary cultures from fronto-parietal cortex and spinal cord of human fetuses.
A) Representative images show that both primary cultures exhibit a prominent positivity for the neuronal marker NeuN (green), while few cells are positive for the glial marker GFAP (red). B) Bar graph shows quantitative analysis of positive cells for each marker, as calculated by counting at least 5 fields from three different slides for each protein. Results are reported as percentage of positive cells over total (magnification 10×).

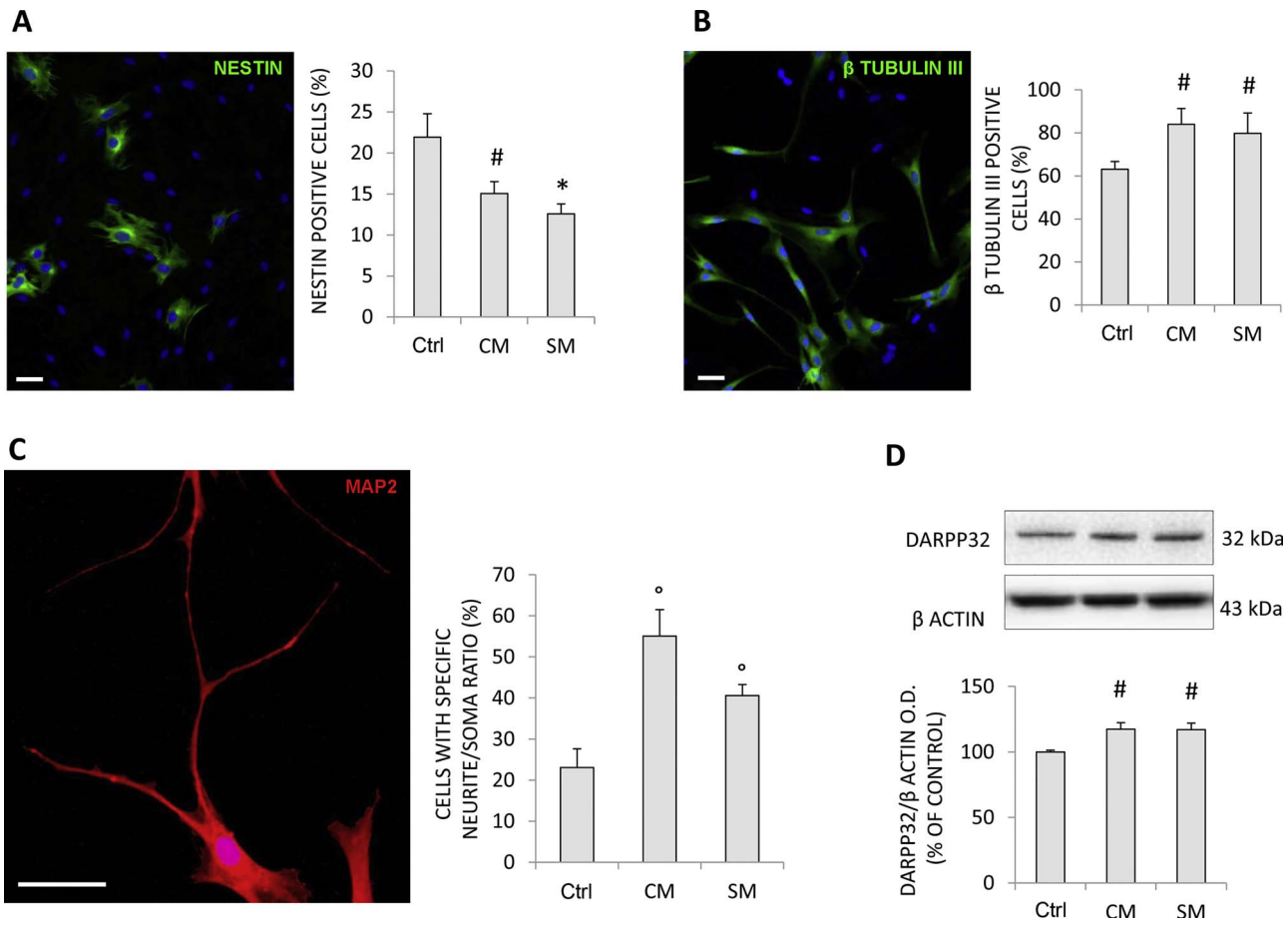

Fig. 3. Effects of the conditioned media on HSP phenotype.

A, B) Representative images of the neural precursor marker nestin (A) and the neuronal marker β tubulin III (B), assessed by immunocytochemistry; the bar graphs show the quantitative analysis of positive cells for each marker, as calculated by counting at least 5 fields from three different slides; results are reported as percentage of positive cells over total (*$p < 0.01$, #$p < 0.05$ *vs* Ctrl; scale bar 50 µm, DAPI counterstained nuclei). C) Representative image of MAP2 immunocytochemical analysis showing neuritogenesis induced by CM and SM; the bar graph indicates the percentage of n-HSP with a neurite length/cell body diameter ratio > 4 (n = 3, °$p < 0.001$ *vs* Ctrl, scale bar 50 µm, DAPI counterstained nuclei). D) Representative western blot image showing enhanced protein level of the striatal marker DARPP32 after treatment with CM and SM; the bar graph shows the computer-assisted quantification of band intensity: data are normalized over β actin signal and are expressed as percentage of control (n = 3, #$p < 0.05$ *vs* Ctrl; O.D., optical density).

cell morphology in terms of neurite outgrowth, which is indicative of neuronal maturation. Hence, neurite outgrowth was determined in MAP2-positive cells by measuring the ratio between the longest neurite length and the cell body diameter and calculating the percentage of cells with a particular ratio, as already described (Sarchielli et al., 2014). As shown in Fig. 3C, in the absence of treatments, about 23% of cells (23.1 ± 4.5%) showed neurites longer than four times the cell body, while the percentage was significantly increased after treatment with CM (55.1 ± 6.4%, $p < 0.001$) and SM (40.6 ± 2.6%, $p < 0.001$). Moreover, with western blot analysis we observed that the protein expression of the striatal marker DARPP32 was significantly increased in HSP grown with CM and SM, when compared to control cells ($p < 0.05$; Fig. 3D).

3.4. Effects of the conditioned media on the n-HSP resting membrane potential

The analysis of the electrophysiological properties of the different HSP cultures obtained from different fetuses aged 9 up to 12 weeks did not evidence any significant difference respective to the different week of gestation. Hence, all data were pooled and reported as the mean ± SEM of all measurements.

The estimation of the RMP indicated that n-HSP (P3/4) in control condition had a mean value of −59.6 ± 3.0 mV (Fig. 1B). To investigate if the conditioned media could affect membrane potential value and improve the excitability, n-HSP cells were cultured in CM and SM for 36 h, before electrophysiological analysis. In any case, by using cells at the same passage for any treatment: we observed a membrane depolarization that was −54 ± 3.2 mV in CM and −31.5 ± 16.2 mV in SM, compared to control values (Fig. 1B). This indicates that the conditioned media had factors capable to shift the RMP towards values closer to the voltage threshold for action potential, and thus increasing the n-HSP intrinsic excitability. However, statistically significant differences were observed under SM treatment, suggesting a major efficacy of this particular medium in causing this effect on RMP.

3.5. Effects of the conditioned media on the n-HSP biophysical properties

The biophysical properties of n-HSP (P3/4) grown in control culture medium (Ctrl) were assed and compared with those of n-HSP cells cultured in CM and SM for 36 h. We first estimated the cell capacitance, C_m, as an index of cell surface (Fig. 1C) bathing the cells with the physiological external solution in the recording chamber and using the voltage clamp mode of our device. We observed that C_m was slightly increased by the type of culture medium, being the measured values: 21.2 ± 4.0, 21.3 ± 5.4 and 22.8 ± 6.1 pF in control medium, in CM and SM, respectively (differences not statistically significant). In contrast, the G_m, index of resting cell membrane permeability was significantly increased in CM (6.2 ± 1.1 nS) and, to a lesser extent, in SM (4.1 ± 0.8 nS) compared to control (2.3 ± 0.7 nS) (Fig. 1F). In

accord, the opposite behavior was observed by the membrane resistance analysis being R_m values: 0.42 ± 0.04, 0.16 ± 0.01 and 0.23 ± 0.02 GΩ, in Ctrl, CM and SM, respectively (Fig. 1E). Consequently, the specific conductance, G_m/C_m, increased in any case compared to control (0.11 ± 0.04 nS/pF), and resulted more altered in CM (0.27 ± 0.07 nS/pF) than in SM (0.17 ± 0.05 nS/pF) (Fig. 1G). In addition, we measured the input resistance values (R_i), somehow reflecting the extent to which membrane channels are open. R_i values turned out to be: 0.36 ± 0.03, 0.07 ± 0.001 and 0.14 ± 0.01 GΩ, in Ctrl, CM and SM, respectively (Fig. 1D). Also the membrane time constant (τ) analysis revealed significant differences among the treatments, increasing from 21.7 ± 2.1 ms in Ctrl, to 32.6 ± 3.2 ms in CM and to 26.1 ± 2.6 ms in SM (Fig. 1H). This seems to suggest that the blend of factors present in CM are more effective in altering the passive membrane properties.

3.6. Effects of the conditioned media on voltage dependent Na^+ currents

We then investigated the occurrence of the main voltage dependent ion currents normally present in neurons. Once again, the results obtained in n-HSP grown in control culture medium were assed and compared with those obtained from n-HSP cells cultured in conditioned media.

Among the number of the voltage-dependent ion currents, outward K^+ currents were regularly recorded (not shown). Since these ion currents are not distinctive features of neurons, we focused our analysis on the inward voltage dependent ion currents that are typically evoked in neuronal cells. Accordingly, to record only Na^+ currents we replaced the physiological bath solution with the 20 mM TEA solution, to avoid the occurrence of K^+ currents. Moreover, we added nifedipine (1 μM) to minimize the occurrence of the high voltage activated L-type Ca^{2+} currents, Ni^{2+} (200 μM) to block T-type current and Cd^{2+} (100 μM) to block all the HVA Ca^{2+} currents. In this condition, we found that all the control n-HSP cells exhibited a TTX-sensitive I_{Na}, as shown in a typical experiment displayed in Fig. 3Aa, with a voltage threshold of about −55 mV. When cells were cultured in both the conditioned media, I_{Na} amplitude resulted increased (Fig. 4A).

The normalized peak current *vs* voltage plot related to all the cells investigated is shown in Fig. 4B: the maximal current amplitude was evoked by the −15 mV step in control cells, but it was evoked by more negative voltages in CM (about −20 mV) and by more positive voltage values in SM (about −5 mV) (Fig. 4a–c). To evaluate the shift of the maximal current amplitude we calculated the steady-state ionic current activation and inactivation curves by eqn 1 and 2 (Fig. 4C). The Boltzmann parameters (listed in Table 1) underwent different changes based on the type of conditioned medium. Values related to I_p/C_m and G_{max}/C_m for I_{Na} are reported in Table 1 as values normalized to the control ones, to better appreciate eventual variations induced by the conditioned media. Culturing the n-HSP cells in CM induced some statistically significant changes in I_{Na} compared to the control medium. The first one consisted of the increase of I_p/C_m and G_{max}/C_m ratios; moreover, the half −voltage activation and inactivation parameters, V_a and V_h, were negatively shifted of about 5 and 4 mV, respectively. In contrast, when the cells were grown in the SM we observed a statistically significant shift of V_a and V_h towards more positive potentials (of 10 and 7 mV, respectively) and a decrease of k_a and k_i values, compared to the control (Table 1).

Table 1
Effect of the conditioned media on the Boltzmann parameters of activation and inactivation curves for I_{Na}.

Parameter	Ctrl	CM	SM
I_p/C_m (Norm)	1.0 ± 0.1	1.2 ± 0.2	1.4 ± 0.2*
G_{max}/C_m (Norm)	1.0 ± 0.1	1.1 ± 0.2	1.5 ± 0.1*,§
V_a (mV)	−30.1 ± 2.9	−34.9 ± 1.1 *	−20.2 ± 1.9 **,§§
k_a (mV)	8.1 ± 0.5	7.8 ± 0.6	7.1 ± 0.5
V_h (mV)	−65 ± 3.1	−69 ± 2.3	−58 ± 3.6 *,§
k_h (mV)	7.5 ± 0.7	7.6 ± 0.7	6.6 ± 0.6
V_{rev} (mV)	46.1 ± 3.7	47.6 ± 4.7	49.1 ± 5.1

I_p/C_m (Norm) and G_{max}/C_m (Norm) data are normalized to Ctrl value. * and ** indicate $p < 0.05$ and < 0.01 *vs* Ctrl; § and §§ indicate $p < 0.05$ and < 0.01 for SM *vs* CM. Data are mean ± SEM. In each experimental condition, data are from 16 to 18 cells.

3.7. Effects of the conditioned media on voltage dependent Ca^{2+} currents

Ca^{2+} channels play key roles in calcium-regulated neuronal functions such as neurotransmitter release and membrane excitability. We can typically discriminate different families of voltage- dependent Ca^{2+} channels based on electrophysiological and pharmacological features: T, L, N and P/Q and R (Bean, 1989; Llinás et al., 1989; Hess, 1990; Tsien et al., 1991; Catterall and Swanson, 2015; Squecco et al., 2016).

To evaluate the presence of functional Ca^{2+} channels, we replaced the physiological bath solution with the TEA-Ca^{2+} bath solution. Then, we applied suitable pulse protocols of stimulation to record the voltage-dependent Ca^{2+} currents, as recently published in our previous characterization of n-HSP cells (Squecco et al., 2016). In the present study,

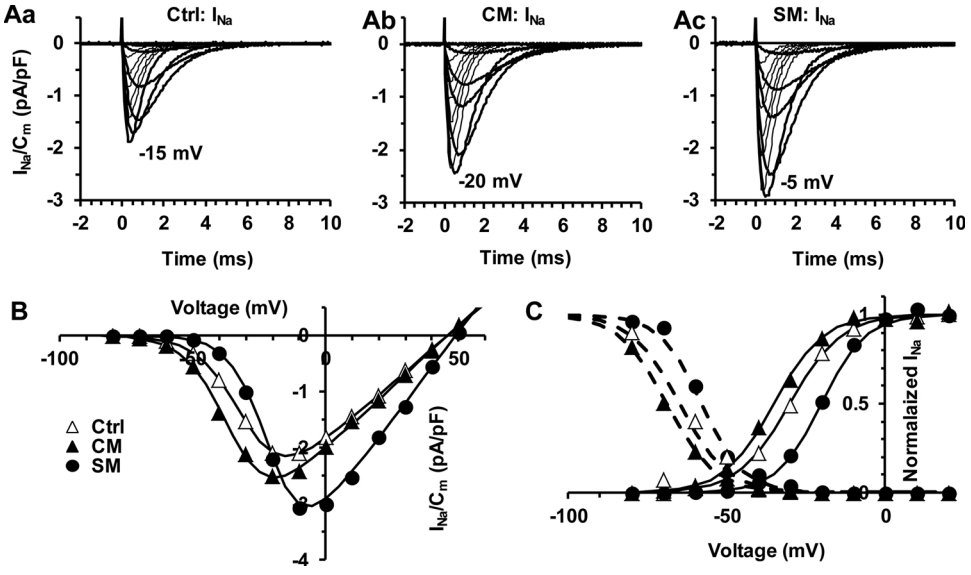

Fig. 4. Inward voltage-dependent Na^+ current is affected by the kind of culture medium.
Representative TTX- sensitive I_{Na} traces from a n-HSP cultured in control medium (Aa), a n-HSP cell grown in CM (Ab) or in SM (Ac); current traces are recorded in 20 mM TEA bath solution and are evoked by depolarizing voltage steps ranging from −70 to 50 mV in 10- mV increments applied from HP = –80 mV. The value of the voltage step eliciting the maximal I_{Na} in any condition is indicated next to the related trace in each panel. B) I–V plots determined at the current peak in n-HSP cells cultured in control medium (open up triangles), CM (filled up triangles), and SM (filled circles). C) Normalized steady – state activation and inactivation curves. The Boltzmann curve for activation (continuous line through the experimental data points) is obtained by the fitting procedure reported in B. The Boltzmann fit is superimposed also on the normalized data related to the inactivation (dashed line). The related Boltzmann parameters ± SEM are listed in Table 1, with the statistical significance. Data are mean values ± SEM; the error bars are not showed for clarity. In each experimental condition, data are from 16 to 18 cells.

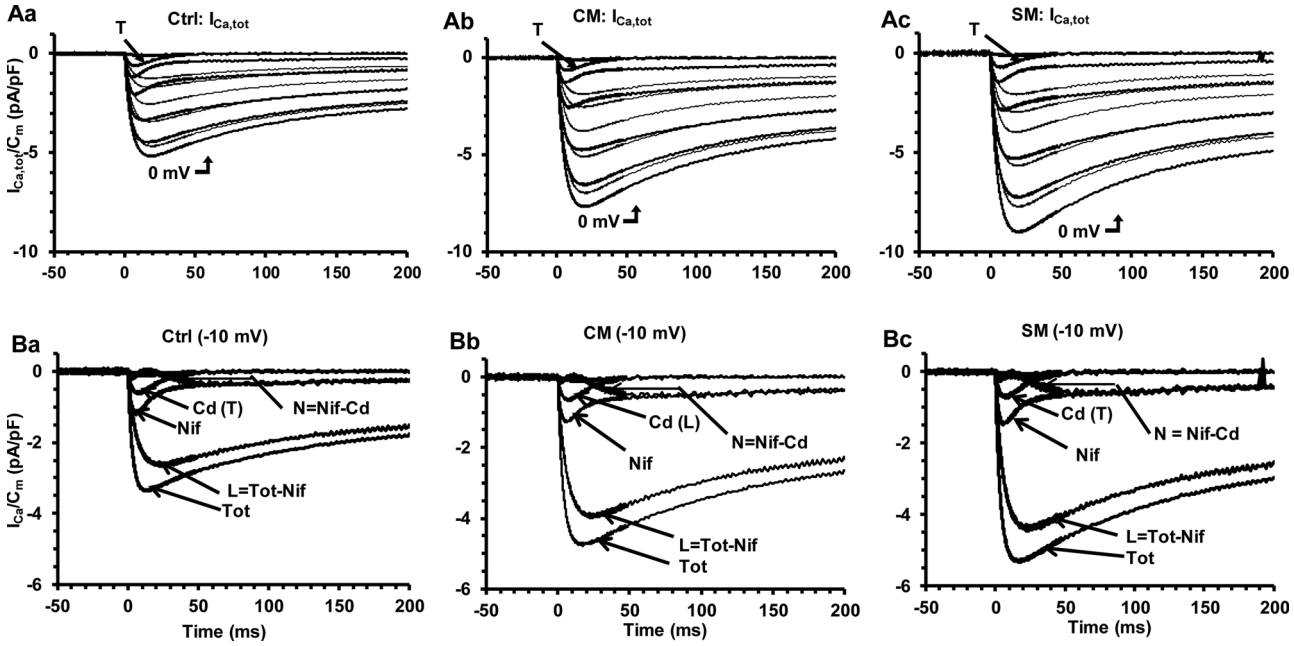

Fig. 5. Time course of Ca^{2+} current and pharmacological dissection.
A) Typical families of $I_{Ca,tot}$ recorded from a n-HSP cell cultured in Ctrl (Aa), CM (Ab) and SM (Ac); the arrows indicate LVA Ca^{2+} current elicited by −50 mV pulses. The voltage pulse eliciting the maximal current amplitude is indicated in each panel next to the corresponding trace (0 mV). B) Pharmacological dissection of $I_{Ca,tot}$ into its different components recorded from a n-HSP cell cultured in Ctrl (Ba), CM (Bb) and SM (Bc). For clarity, in each panel only the current trace evoked by the −10 mV voltage pulse (HP = –80 mV) is depicted for any recording condition.

all our n-HSP cells showed voltage dependent Ca^{2+} currents (Fig. 5), mostly consisting of two main components. The first was a low voltage-activated (LVA) inward transient current that was recorded from −60/50 mV (indicated by the arrow in panels A). The second was a high-voltage-activated (HVA), slowly activating and inactivating current, that appeared from −40/–30 mV and superimposed on the transient one. To further discriminate the different components of Ca^{2+} currents we used a pharmacological dissection (Fig. 5B). For clarity, only the current trace evoked by the −10 mV step for any recording condition is displayed in panels B of this figure. The specific total Ca^{2+} current trace (I_{tot}/C_m) recorded by a cell cultured in control condition (Ctrl) is shown in panel 5Ba; adding nifedipine to the bath solution caused the appearance of a transient current (Nif), but did not block the HVA type current completely. In fact, a slow decaying residual current (about the 10% of the control) could still be observed in the presence of nifedipine. Then, by subtracting Nif- from Tot- trace, we mathematically obtained the nifedipine-sensitive L-type Ca^{2+} current (L = Tot-Nif). Adding Cd^{2+} to the external solution completely blocked HVA-type current. By subtracting the current trace obtained in the presence of Cd^{2+} from that obtained in the presence of nifedipine (Nif-Cd) we could obtain the N-type Ca^{2+} current.

Therefore, we can assess that neither Cd^{2+} nor nifedipine added to the external bath solution, affected the LVA transient current, confirming the occurrence of the T-type currents. Moreover, the observed HVA Ca^{2+} currents mainly consisted of the L-type nifedipine-sensitive one, whereas a smaller fraction was due to the other Ca^{2+} channels such as N −type ones (Fig. 5B). However, the other HVA Ca^{2+} currents (P/Q- and R- types) were hardly analysable since the residual current observed after the N-type channel blocker application was very small in size or completely absent. The same procedure was followed for cells maintained in SM (Fig. 5Bb) and CM (Fig. 5Bc). The total Ca^{2+} currents evoked in the cells cultured in CM showed an increased amplitude (Fig. 5Ab) compared to those grown in Ctrl (Fig. 5Aa). This increase was even more evident in the cells maintained in SM (Fig. 5Ac).

We then examined the three different components separately and the results are shown in Figs. 6–8, for T-, L- and N-type Ca^{2+} currents, respectively.

The analysis of T- type current time course is shown in Fig. 6A, where the representative families of traces are recorded from n-HSP cells maintained in the three different conditions (panels Aa, Ab and Ac). When the cells were treated both with the CM (panel Ab) and SM (panel Ac) we consistently observed a small increase of the specific $I_{Ca,T}$ compared to Ctrl (panel Aa). We then calculated the normalized I–V plots, by evaluating the mean current values evoked by any voltage step and dividing it for the cell capacitance (Fig. 6B). We also evaluated the activation and inactivation curves and the corresponding normalized Boltzmann curves (Fig. 6C). Again, some Boltzmann parameters were differently altered by the type of the conditioned medium used (Table 2). The n-HSP cultured in CM or SM showed substantial variations of $I_{Ca,T}$ compared to control, consisting of an increase of the related I_p/C_m and G_{max}/C_m ratios, and a shift of both V_a and V_h values towards more negative potential, in contrast to the effect observed for I_{Na}. The parameter values and statistical significance are displayed in Table 2. The time constant values, τ_a and τ_i, did not show statistically significant differences at any voltage investigated in the three different conditions. In fact, for the −20 mV step τ_a was 3.1 ± 0.4 ms in Ctrl, 3.0 ± 0.4 in CM and 2.8 ± 0.4 ms in SM. Similarly, τ_i values were 10.2 ± 1.1, 9.2 ± 0.9 and 9.3 ± 1.0 ms for Ctrl, CM and SM, respectively.

The analysis of L- type current time course is shown in Fig. 7, where typical families of traces recorded from n-HSP cells maintained in Ctrl medium, in CM and SM are displayed in panel Aa, Ab and Ac, respectively. Cells treated with both the CM and SM conditioned media consistently showed a strong increase of $I_{Ca,L}$ compared to that recorded from Ctrl cells. Particularly, n-HSP cells cultured in CM showed variations of $I_{Ca,L}$ features compared to control such as an increase of G_{max}/C_m and a shift of V_a and V_h values towards more negative potential (about 3 and 6 mV, respectively). When n-HSP cells were cultured in SM, they showed statistically significant differences compared to control and also with CM. In fact, in these cells we observed a positive shift of V_a of about 4 mV compared to control, that is in the opposite direction compared to CM. Also V_h was positively shifted compared to control. All the parameter values and statistical significance are displayed in Table 2. Once again, the τ_a and τ_i values did not show

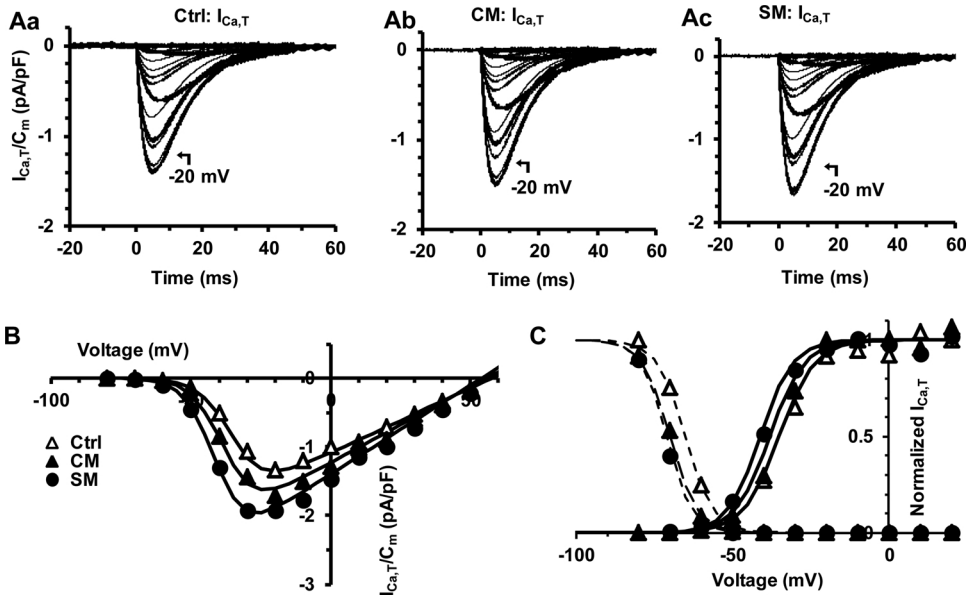

Fig. 6. Effect of the conditioned media on T-type Ca^{2+} currents.
Typical families of T-type Ca^{2+} currents (obtained as explained in Materials and Methods section), recorded from n-HSP cells maintained in Ctrl condition (Aa), in CM (Ab) and in SM (Ac); the voltage pulse eliciting the maximal current amplitude is indicated in each panel next to the related trace (–20 mV). B) I–V plots determined at the current peak in n-HSP cells cultured in control medium (open up triangles), CM (filled up triangles), and SM (filled circles). C <) Normalized steady–state activation (continuous line) and inactivation curves (dashed line). The related Boltzmann parameters ± SEM are listed in Table 2, with the statistical significance. B, C <) Data are mean values ± SEM (error bar not showed for clarity). In each experimental condition, data are from 18 to 20 cells.

statistically significant differences at any voltage investigated in the three different conditions. In fact, for the 0 mV step τ_a was 7.0 ± 0.8 ms in Ctrl, 7.2 ± 0.9 in CM and 7.0 ± 0.9 ms in SM. Similarly, τ_i values were 90.6 ± 10, 85.3 ± 9 and 87.1 ± 9 ms for Ctrl, CM and SM, respectively.

The time course of the N-type current is displayed in Fig. 8A, that again shows the typical families of traces recorded from a n-HSP cell maintained in Ctrl (Aa), in CM (Ab) and SM (Ac). Cells treated with the CM and SM conditioned media consistently showed a strong increase of the specific $I_{Ca,N}$ compared to Ctrl. Particularly, n-HSP cells cultured in CM exhibited peculiar variations of $I_{Ca,N}$ compared to control such as an increase of G_{max}/C_m and a shift of V_a value towards more negative potentials. The n-HSP cells cultured in SM displayed statistically significant differences compared to control and also to CM (parameters and statistical significance listed in Table 2). Notably, the maximal specific current amplitude, I_{Ca}/C_m, of T-type was more markedly affected by SM than by CM, that of L- type was more markedly affected by CM than by SM, whereas the N-type Ca^{2+} current was similarly enhanced by both media.

In contrast, when we considered the related maximal current amplitude value, I_{Ca}, we could clearly observe that SM caused a more significant enhancement in amplitude of all the Ca^{2+} current types examined compared to CM (Fig. 9).

4. Discussion

The processes governing neuronal growth, migration and differentiation include a complex interplay of various external factors, such as hormones, neurotransmitters or peptides (growth factors), which are present in the surrounding milieu (Sariola and Saarma, 2003; Moody

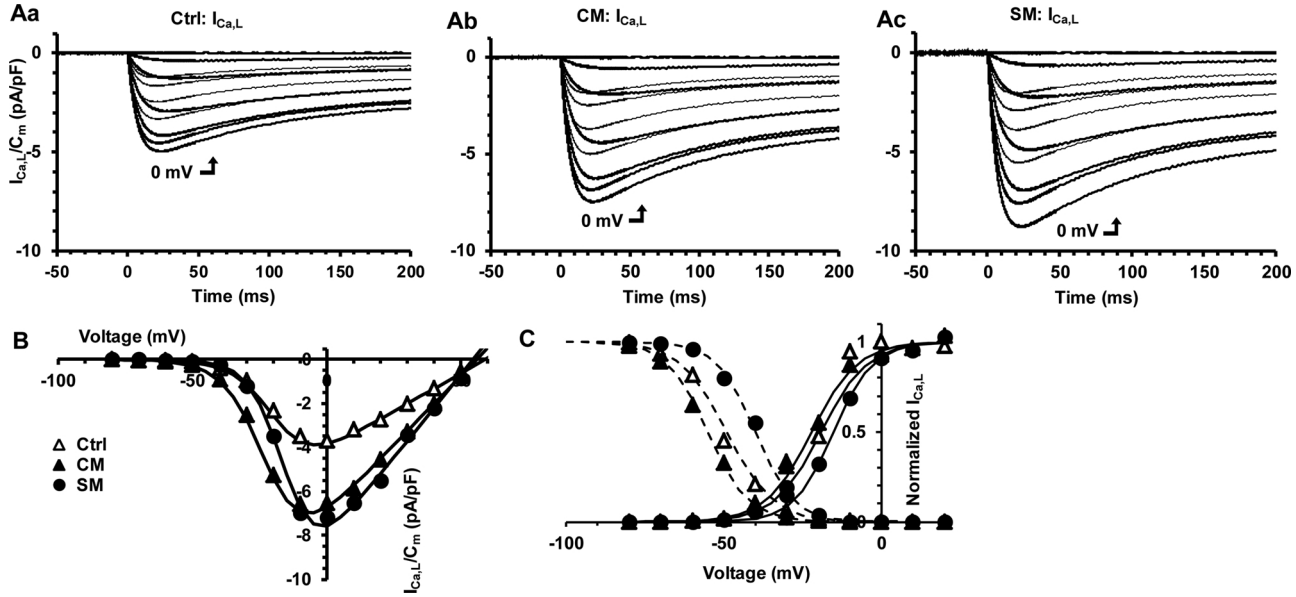

Fig. 7. Effect of the conditioned media on L-type Ca^{2+} currents.
Typical families of L-type Ca^{2+} currents obtained by pharmacological dissection as explained in Fig. 5B from n-HSP cells maintained in Ctrl condition (Aa), in CM (Ab) and in SM (Ac); the voltage pulse eliciting the maximal amplitude is indicated in each panel next to the related trace (0 mV). B) I–V plots determined at the current peak in n-HSP cells cultured in Ctrl medium (open up triangles), CM (filled up triangles), and SM (filled circles). C <) Normalized steady – state activation (continuous line) and inactivation curves (dashed line). The related Boltzmann parameters, mean ± SEM, are listed in Table 2, with the statistical significance. B, C <) Data are mean values (error bar not shown). Same cells as in Fig. 6.

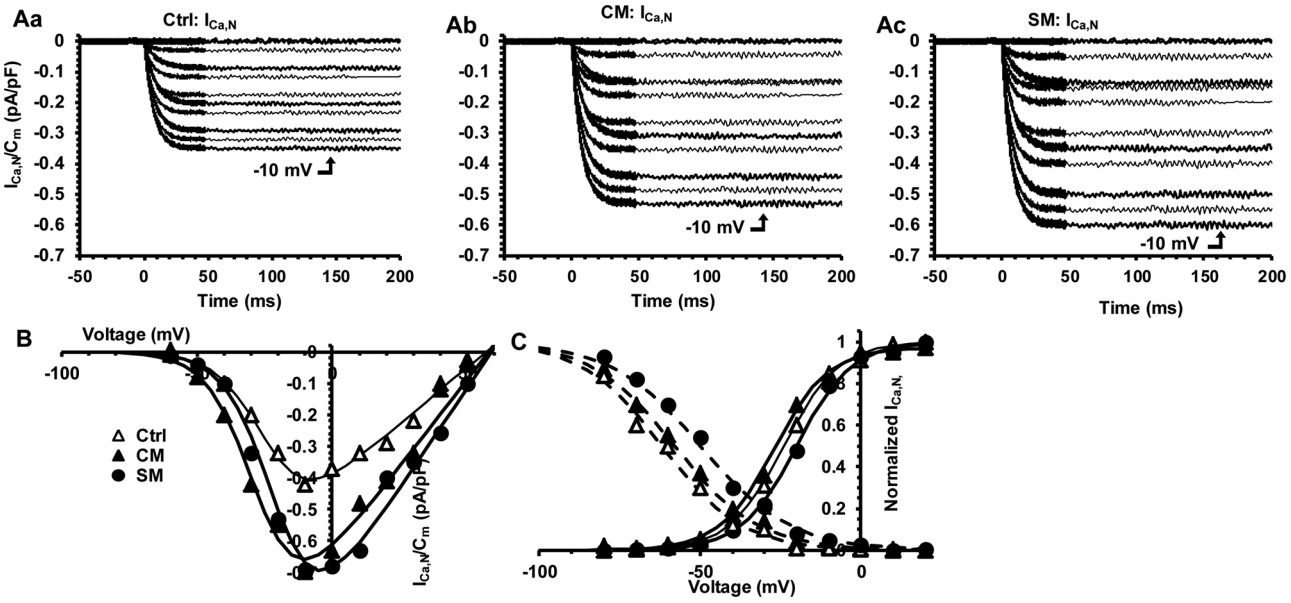

Fig. 8. Effect of the conditioned media on N-type Ca^{2+} currents.
Typical families of N-type Ca^{2+} currents obtained by pharmacological dissection as explained in Fig. 3B from n-HSP cells maintained in Ctrl condition (Aa), in CM (Ab) and in SM (Ac); the voltage pulse eliciting the maximal amplitude is indicated in each panel next to the related trace (–10 mV). B) I–V plots determined at the current peak in n-HSP cells cultured in Ctrl medium (open up triangles), CM (filled up triangles), and SM (filled circles). C <) Normalized steady-state activation (continuous line) and inactivation curves (dashed line). The related Boltzmann parameters ± SEM are listed in Table 2, with the statistical significance. B, C <) Data are mean values ± SEM (error bar not shown). Same cells as in Fig. 6.

Table 2
Effect of the conditioned media on the Boltzmann parameters of activation and inactivation curves for $I_{Ca,T}$, $I_{Ca,L}$ and $I_{Ca,N}$.

Parameter	Ctrl	CM	SM
$I_{Ca,T}$			
I_p/C_m (Norm)	1.0 ± 0.1	1.2 ± 0.1	1.5 ± 0.2*
G_{max}/C_m (Norm)	1.0 ± 0.1	1.3 ± 0.1*	1.6 ± 0.1 *,§
V_a (mV)	−35 ± 3.2	−38 ± 3.2	−41 ± 3.8
k_a (mV)	5.5 ± 0.4	5.5 ± 0.4	5.2 ± 0.4
V_h (mV)	−65 ± 5.1	−70 ± 5.6	−71 ± 5.6
k_h (mV)	4.5 ± 0.4	4.4 ± 0.4	4.1 ± 0.3
V_{rev} (mV)	−58 ± 6.1	−56 ± 5.5	−54 ± 5.8
$I_{Ca,L}$			
I_p/C_m (Norm)	1.0 ± 0.1	2.0 ± 0.2 **	1.9 ± 0.2 **
G_{max}/C_m (Norm)	1.0 ± 0.1	1.8 ± 0.2 **	2.2 ± 0.2 ***
V_a (mV)	−19 ± 1.6	−22 ± 1.7*	−15 ± 1.4 *,§§
k_a (mV)	7.5 ± 0.5	7.4 ± 0.5	6.3 ± 0.4 *,§
V_h (mV)	−49 ± 4.7	−55 ± 5.1	−40 ± 3.8**,§§
k_h (mV)	7.4 ± 0.7	6.5 ± 0.6	6.1 ± 0.6
V_{rev} (mV)	58.9 ± 4.7	56.5 ± 5.5	56.4 ± 5.6
$I_{Ca,N}$			
I_p/C_m (Norm)	1.0 ± 0.1	1.7 ± 0.2 ***	1.7 ± 0.3 ***
G_{max}/C_m (Norm)	1.0 ± 0.1	1.5 ± 0.2 **	1.8 ± 0.2 ***
V_a (mV)	−24.0 ± 1.6	−26.6 ± 2.7	−19.8 ± 1.4 *,§
k_a (mV)	8.5 ± 0.5	8.5 ± 0.5	8.6 ± 0.5
V_h (mV)	−62 ± 4.7	−58 ± 4.3	−50 ± 3.8**,§
k_h (mV)	12.5 ± 1.1	13.1 ± 1.3	14.1 ± 1.3
V_{rev} (mV)	49.5 ± 4.1	49.1 ± 5.3	49.3 ± 5.2

Parameters as in Table 1. *, ** and *** indicate $p < 0.05$, < 0.01 and < 0.001 *vs* control; § and §§ indicate $p < 0.05$ and < 0.01 for SM *vs* CM medium. In each experimental condition, data are from 18 to 20 cells.

and Bosma, 2005; Bouron et al., 2006; Zuccato et al., 2010; Yuzwa et al., 2016). During these processes, the above factors can modify the functionality and/or the expression of different ionic channels, such as Na^+ and Ca^{2+}, depending on the type of neuron, the presynaptic or postsynaptic localization and the stage of differentiation (Westerlund et al., 1993; Colston et al., 1998; Joux et al., 2001; Ji et al., 2010). Thus, the HSP cells cultured with neuronal conditioned medium may specifically differentiate and alter their biophysical properties according to the type of inductive medium used.

In this regard, we have investigated, for the first time to our knowledge, the effects of cortical and spinal cord conditioned media on the differentiation potential of HSP cells. Our recent previous researches suggested that these cells are quite immature neuron-like cells (Sarchielli et al., 2014; Squecco et al., 2016), mainly expressing the neuronal progenitor marker β-tubulin III (Sarchielli et al., 2014 and present study), and the present electrophysiological study confirms this finding since they showed very small Na^+ and Ca^{2+} currents. However, HSPs although immature are already committed toward the specific striatal phenotype and accordingly, also express DARPP32 (Sarchielli et al., 2014 and present study). More importantly, we previously demonstrated the ability of HSPs to differentiate in response to neurotrophins, such as BDNF and FGF2 (Sarchielli 2014, Squecco 2016). Here we show that more composite culture media, such as CM and SM, which more properly reflect the complexity of an *in vivo* milieu, may drive HSP maturation both in terms of phenotypic (neurite outgrowth, expression of the striatal marker DARPP32) and electrophysiological (membrane parameters, intrinsic excitability, ion current amplitude and kinetics) properties.

Our results demonstrate that the biophysical properties of n-HSP cells were substantially modified when maintained in CM or SM, as compared to Ctrl medium. We have shown that both the conditioned media affected the RMP altering the cell excitability, decreased the input resistance and increased the membrane conductance and the membrane time constant values. Particularly, both the conditioned media, while significantly reducing the input resistance of the n-HSP cells that reflects the extent to which membrane channels are open, were able to increase the opening of ionic channels at resting potential, in accord with the estimated higher conductance compared to Ctrl condition. Moreover, the analysis of the membrane time constant, a commonly used way of measuring how quickly a neuron's voltage level decays to its resting state after it receives an input signal, indicates that both SM and, most of all, the CM were able to prolong the depolarized state of the cells, further improving their intrinsic excitability.

Although not statistically significant, the inductive media increased the cell capacitance and this finding is in agreement with the induction of the neurites outgrowth. In fact, as already observed in our previous

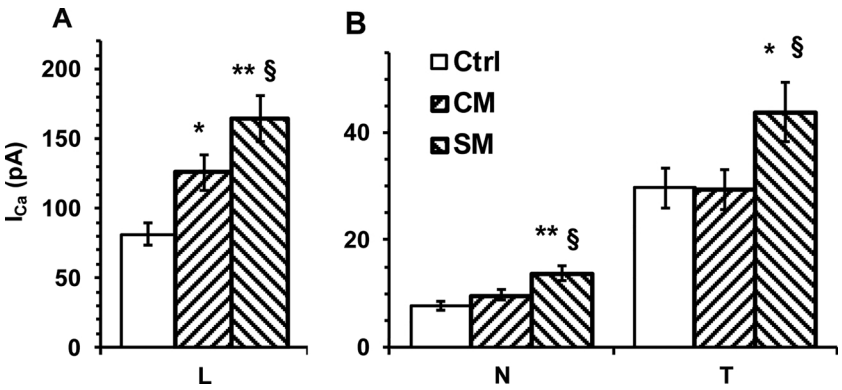

Fig. 9. Different effect of the conditioned media on L-, N- and T-type Ca^{2+} currents.
The maximal current amplitude (I_{Ca}) is significantly enhanced in SM compared to CM for all the Ca^{2+} current types. * and ** indicate $p < 0.05$ and $p < 0.01$ *vs* the related control (Ctrl); § indicate $p < 0.05$ of SM *vs* CM. Data are from the same cells of Figs. 6–9. Values are mean ± SEM. Note the different ordinate scale of panels A and B.

paper (Luciani et al., 2010) the newly forming protrusions require the addition of new membrane surface and this justifies the trend of an increased membrane capacitance. Another significant effect induced by the conditioned media was observed on the main inward cationic current, whose amplitudes and conductance resulted increased, but with different changes in current kinetics. The analysis of all the inward currents suggested that cells kept in CM acquired a sort of enhanced excitability compared to those maintained in Ctrl medium. Indeed, in CM cultured cells the V_a parameter of all the inward currents, such as $I_{Na,}$ T-, L- and N-type I_{Ca} was shifted towards more negative potentials, thus suggesting that voltage-dependent cation channels may be activated at a lower voltage threshold compared to control cultures. In contrast, the cells maintained in SM showed inward currents, except for the T-type Ca^{2+} current, with an opposite kinetic behaviour. In fact, the window of membrane potentials where Na^+, L- and N-type Ca^{2+} channels are simultaneously activated and not completely inactivated was positively shifted when the cells were grown in SM, showing in any case a higher voltage of half-maximal activation.

The effects of the conditioned media that we observed on n-HSP cells in the present study somehow differ from those previously observed from our research group (Squecco et al., 2016). In fact, culturing human n-HSP cells in a medium containing only one kind of neurotrophin (such as FGF2 or BDNF), only caused a decrease of L- and T-type Ca^{2+} current size without affecting the V_a parameters (Squecco et al., 2016). As well, the dopaminergic agonist SKF82958 or quinpirole selective for D1- and D2-dopamine receptors, respectively, acutely applied to the bath solution, induced a slight membrane hyperpolarization and reduced in amplitude both L- and N-type but unaffected T-type Ca^{2+} currents (Squecco et al., 2016). Otherwise, Bouron et al. (2006) found that glutamate and BDNF decreased Ca^{2+} current in cortical neurons isolated from embryonic day 13 (E13) mouse fetuses, suggesting that this down-regulation of I_{Ca} could exert a neuroprotective action on embryonic cortical neurons. In contrast, we have found that culturing human n-HSP cells in CM and SM causes an increase of Na^+ and Ca^{2+} influx, but we have to consider that our cells in control condition (without any peculiar treatment) elicit I_{Na} and I_{Ca} of a small amplitude, suggesting a low degree of differentiation. Notably, stem cells poorly express the inward voltage dependent I_{Na} and I_{Ca}; therefore, the increase of the expression/functionality as well as the specific type of voltage dependent Na^+ and Ca^{2+} channel isoforms expressed can be indicative of an improved differentiation. In line with this view, D'Ascenzo et al. (2006) showed that the increase of I_{Ca} allowed a better differentiation in stem/progenitor cells derived from the brain cortex of postnatal mice.

In the present research, the observed changes of the ion channels voltage dependence may be due to the modulation of the existing Na^+ and Ca^{2+} channels due to growth factors, neurotransmitters and intracellular signals present in the different conditioned media. However, we should also consider the possibility that the different conditioned media could induce the expression of diverse channel isoforms. For instance, the different voltage-gated sodium channels identified in mammals have specific developmental, tissue or cellular distributions and their peculiar kinetics and voltage-dependent properties may have a role in determining the integrative and excitability properties of neurons (Goldin, 2001).

Notably, the different electrophysiological results obtained in n-HSP cells cultured in control medium compared to those obtained in the conditioned media and those between the two different conditioned media strongly suggest that the peculiar observed changes in I_{Na} and I_{Ca} Boltzmann parameters were actually due to neurotrophins, growth factors, neurotransmitters or signaling molecules specifically released by the neuronal population of origin. Among the mechanisms that control the neuronal development, signaling of major neurotransmitters such as γ-aminobutyric acid and glutamate seems to play a key role and thus deserves further investigation to verify their contribute to the enhanced excitability of the immature brain (Sanchez and Jensen, 2001). Moreover, the identification of the factors in the conditioned medium that caused the electrophysiological and morphological changes in HSPs, as well as the possible changes in gene and protein expression profiles remain to be clarified. Future studies will be focused on the explanation of these mechanisms.

5. Conclusions

In conclusion, we suggest that culturing n-HSP cells in neuronal (cortical or spinal cord) conditioned media gradually helps in acquiring inward ion currents with different kinetics typical of neurons that are more excitable. This indicates that changes occurring in cell microenvironment, such as the presence of certain neurotransmitters, growth or specific signalling factors actually influence HSP cells differentiation < *in vitro* (Colston et al., 1998; Bouron et al., 2006; Yuzwa et al., 2016). Although both conditioned media are able to direct the n-HSP cells towards an enhanced excitability, our functional findings indicate that the bulk of n-HSP acquire a phenotype better resembling to mature striatal neurons in a different manner in response to the cortical or spinal inductive stimuli. Principally, when n-HSPwere treated with the spinal medium they showed peculiar kinetics and an increased amplitude of Na^+ current as well as L and N- type Ca^{2+} currents; they also showed a significantly more depolarized membrane potential. In contrast, when cells were cultured in the cortical medium they mainly exhibited a significant and more marked increase of the membrane conductance and time constant values. Overall, these data confirm the plasticity of fetal neuronal precursors already committed toward a specific neuronal phenotype, but also functionally modifiable according to environmental cues, a crucial issue when considering cell-based therapies for neuronal tissue repair. However, future studies should be carried out to clarify their effective capability to differentiate into fully functional neurons with a specific phenotype. As well, possible results of *in vivo* experiments would greatly enhance the importance of this research.

Conflict of interests

None.

Author contributions

R.S., F.F., G.V., P.G. and A.M. designed the study; E.I., R.S., R.G. and M.C.B. made electrophysiological experiments; E.S. and A.M. made cell cultures, western blot and Immunofluorescence analysis; all authors contributed to acquisition, analysis or interpretation of data for the work; all were involved in drafting the work. R.S., F.F., G.V. and A.M. revised it critically for important intellectual content. All authors approved the final version of the manuscript and agree to be accountable for all aspects of the work in ensuring that questions related to the accuracy or integrity of any part of the work are appropriately investigated and resolved. All persons designated as authors qualify for authorship, and all those who qualify for authorship are listed.

Ethics statement

Neuronal samples were obtained from 9 to 12 week-old legally aborted fetuses, according to the ethical guidelines of the Italian National Institute of Health. The use of human fetal tissue for research purposes was approved by the National Ethics Committee and the Committee for investigation in Humans of the University of Florence (Protocol n° 678304).

Declare

No conflict of interests.

Acknowledgements

The authors wish to thank Ente Cassa di Risparmio di Firenze for supporting this research (ECRF n. 2012.0621). This research has been funded by University of Florence, Grant no ROBERTASQUECCORICATEN14 to RS.

References

Ambrosini, S., Sarchielli, E., Comeglio, P., Porfirio, B., Gallina, P., Morelli, A., Vannelli, G.B., 2015. Fibroblast Growth Factor and Endothelin-1 receptors mediate the response of human striatal precursor cells to hypoxia. Neuroscience 289, 123–133.

Bean, B.P., 1989. Neurotransmitter inhibition of neuronal calcium currents by changes in channel voltage dependence. Nature 340, 153–156.

Bouron, A., Boisseau, S., De Waard, M., Peris, L., 2006. Differential down-regulation of voltage-gated calcium channel currents by glutamate and BDNF in embryonic cortical neurons. Eur. J. Neurosci. 24, 699–708.

Catterall, W.A., Swanson, T.M., 2015. Structural basis for pharmacology of voltage-gated sodium and calcium channels. Mol. Pharmacol. 88, 141–150.

Clelland, C.D., Barker, R.A., Watts, C., 2008. Cell therapy in Huntington disease. Neurosurg. Focus 24, 3–4.

Colston, J.T., Valdes, J.J., Chambers, J.P., 1998. Ca^{2+} (1-subunit transcripts are differentially expressed in rat pheochromocytoma (PC12) cells following nerve growth factor treatment. Int. J. Dev. Neurosci. 16, 379–389.

Crescioli, C., Squecco, R., Cosmi, L., Sottili, M., Gelmini, S., Borgogni, E., Sarchielli, E., Scolletta, S., Francini, F., Annunziato, F., Vannelli, G.B., Serio, M., 2008. Immunosuppression in cardiac graft rejection: a human in vitro model to study the potential use of new immunomodulatory drugs. Exp. Cell Res. 314, 1337–1350.

D'Ascenzo, M., Piacentini, R., Casalbore, P., Budoni, M., Pallini, R., Azzena, G.B., Grassi, C., 2006. Role of L-type Ca^{2+} channels in neural stem/progenitor cell differentiation. Eur. J. Neurosci. 23, 935–944.

Di Franco, A., Guasti, D., Squecco, R., Mazzanti, B., Rossi, F., Idrizaj, E., Gallego-Escuredo, J.M., Villarroya, F., Bani, D., Forti, G., Vannelli, G., Luconi, M., 2016. Searching for classical brown fat in humans: development of a novel human fetal brown stem cell model. Stem Cells 34, 1679–1691.

Evans, A.E., Kelly, C.M., Precious, S.V., Rosser, A.E., 2012. Molecular regulation of striatal development: a review. Anat. Res. Int. 2012, 106529. http://dx.doi.org/10.1155/2012/106529. 14 pages.

Gallina, P., Paganini, M., Lombardini, L., Mascalchi, M., Porfirio, B., Gadda, D., Marini, M., pinzani, P., Salvianti, F., Crescioli, C., Bucciantini, S., machi, C., Sarchielli, E., Romoli, A.M., Bestini, E., Urbani, S., Bartolozzi, B., De Cristofaro, M.T., Piacentini, S., Saccaridi, P., Pupi, A., Vannelli, G.B., Di Lorenzo, N., 2010. Human striatal neuroblasts develop and build a striatal-like structure into the brain of Huntington's disease patients after transplantation. Exp. Neurol. 222, 30–41.

Goldin, A.L., 2001. Resurgence of sodium channel research. Ann. Rev. Physiol. 63, 871–894.

Gustafson, N., Gireesh-Dharmaraj, E., Czubayko, U., Blackwell, K.T., Plenz, D., 2006. A comparative voltage and current-Clamp analysis of feedback and feedforward synaptic transmission in the striatal microcircuit in vitro. J. Neurophysiol. 95, 737–752.

Hess, P., 1990. Calcium channels in vertebrate cells. Ann. Rev. Neurosci. 13, 337–356.

Heubach, J.F., Graf, E.M., Leutheuser, J., Bock, M., Balana, B., Zahanich, I., Christ, T., Boxberger, S., Wettwer, E., Ravens, U., 2004. Electrophysiological properties of human mesenchymal stem cells. J. Physiol. 554, 659–672.

Ji, Y., Lu, Y., Yang, F., Shen, W., Tang, T.T., Feng, L., Duan, S., Lu, B., 2010. Acute and gradual increases in BDNF concentration elicit distinct signaling and functions in neurons. Nat. Neurosci. 13, 302–309.

Joux, N., Chevaleyre, V., Alonso, G., Boissin-Agasse, L., Moos, F.C., Desarménien, M.G., Hussy, N.N., 2001. High voltage-activated Ca^{2+} currents in rat supraoptic neurones: biophysical properties and expression of the various channel α1 subunits. J. Neuroendocrinol. 13, 638–649.

Li, G.R., Sun, H., Deng, X., Lau, C.P., 2005. Characterization of ionic currents in human mesenchymal stem cells from bone marrow. Stem Cells 23, 371–382.

Llinás, R.R., Sugimori, M., Cherksey, B., 1989. Voltage-dependent calcium conductances in mammalian neurons. The P channel. Ann. N. Y. Acad. Sci. 560, 103–111.

Luciani, P., Deledda, C., Benvenuti, S., Cellai, I., Squecco, R., Monici, M., Cialdai, F., Luciani, G., Danza, G., Di Stefano, C., Francini, F., Peri, A., 2010. Differentiating effects of the glucagon-like peptide-1 analogue exendin-4 in a human neuronal cell model. Cell. Mol. Life Sci. 67, 3711–3723.

Moe, M.C., Varghese, M., Danilov, A.I., Westerlund, U., Ramm-Pettersen, J., Brundin, L., Svensson, M., Berg-Johnsen, J., Langmoen, I.A., 2005. Multipotent progenitor cells from the adult human brain: neurophysiological differentiation to mature neurons. Brain 128, 2189–2199.

Moody, W.J., Bosma, M.M., 2005. Ion channel development, spontaneous activity, and activity-dependent development in nerve and muscle cells. Physiol. Rev. 85, 883–941.

Novak, M.J., Tabrizi, S.J., 2010. Huntington's disease. BMJ 340, c3109. http://dx.doi.org/10.1136/bmj.c3109.

Onorati, M., Castiglioni, V., Biasci, D., Cesana, E., Menon, R., Vuono, R., Talpo, F., Laguna Goya, R., Lyons, P.A., Bulfamante, G.P., Muzio, L., Martino, G., Toselli, M., Farina, C., Barker, R.A., Biella, G., Cattaneo, E., 2014. Molecular and functional definition of the developing human striatum. Nat. Neurosci. 17, 1804–1815.

Paganini, M., Biggeri, A., Romoli, A.M., Mechi, C., Ghelli, E., Berti, V., Pradella, S., Bucciantini, S., Catelan, D., Saccaridi, R., Bombardini, L., Ma scalchi, M., Massacesi, L., Porfirio, B., Di Lorenzo, N., Vannelli, G.B., Gallina, P., 2014. Fetal striatal grafting slows motor and cognitive decline of Huntington's disease. J. Neurol. Neurosurg. Psychiatry 85, 974–981.

Pauly, M.C., Piroth, T., Döbrössy, M., Nikkhah, G., 2012. Restoration of the striatal circuitry: from developmental aspects toward clinical applications. Front. Cell. Neurosci. 6, 16.

Peschanski, M., Cesaro, P., Hantraye, P., 1995. Rationale for intrastriatal grafting of striatal neuroblasts in patients with Huntington's disease. Neuroscience 68, 273–285.

Picken Bahrey, H.L., Moody, W.J., 2003. Early development of voltage-gated ion currents and firing properties in neurons of the mouse cerebral cortex. J. Neurophysiol. 89, 1761–1773.

Plotkin, J.L., Wu, N., Chesselet, M.F., Levine, M.S., 2005. Functional and molecular development of striatal fast-spiking GABAergic interneurons and their cortical inputs. Eur. J. Neurosci. 22, 1097–1108.

Sanchez, R.M., Jensen, F.E., 2001. Maturational aspects of epilepsy mechanisms and consequences for the immature brain. Epilepsia 42, 577–585.

Sarchielli, E., Marini, M., Ambrosini, S., Peri, A., Mazzanti, B., Pinzani, P., Barletta, E., Ballerini, L., Paternostro, F., Paganini, M., Porfirio, B., Morelli, A., Gallina, P., Vannelli, G.B., 2014. Multifaceted roles of BDNF and FGF2 in human striatal primordium development. An in vitro study. Exp. Neurol. 257, 130–147.

Sariola, H., Saarma, M., 2003. Novel functions and signalling pathways for GDNF. J. Cell Sci. 116, 3855–3862.

Sartiani, L., Bettiol, E., Stillitano, F., Mugelli, A., Cerbai, E., Jaconi, M.E., 2007. Developmental changes in cardiomyocytes differentiated from human embryonic stem cells: a molecular and electrophysiological approach. Stem Cells 25, 1136–1144.

Squecco, R., Idrizaj, E., Morelli, A., Gallina, P., Vannelli, G.B., Francini, F., 2016. An electrophysiological study on the effects of BDNF and FGF2 on voltage dependent Ca^{2+} currents in developing human striatal primordium. Mol. Cell. Neurosci. 75, 50–62.

Tsien, R.W., Ellinor, P.T., Horne, W.A., 1991. Molecular diversity of voltage-dependent Ca^{2+} channels. Trends Pharmacol. Sci. 12, 349–354.

Ulfig, N., 2000. The ganglionic eminence-new vistas. Trends Neurosci. 23, 530.

Westerlund, U., Moe, M.C., Varghese, M., Berg-Johnsen, J., Ohlsson, M., Langmoen, I.A., Yang, J., Tsien, R.W., 1993. Enhancement of N- and L-type calcium channel currents by protein kinase C in frog sympathetic neurons. Neuron 10, 127–136.

Westerlund, U., Moe, M.C., Varghese, M., Berg-Johnsen, J., Ohlsson, M., Langmoen, I.A., Svensson, M., 2003. Stem cells from the adult human brain develop into functional neurons in culture. Exp. Cell Res. 289, 378–383.

Yuzwa, S.A., Yang, G., Borrett, M.J., Clarke, G., Cancino, G.I., Zahr, S.K., 2016. Proneurogenic ligands defined by modeling developing cortex growth factor communication networks. Neuron 91, 988–1004.

Zuccato, C., Valenza, M., Cattaneo, E., 2010. Molecular mechanisms and potential therapeutical targets in Huntington's disease. Physiol. Rev. 90, 905–981.